

# Effect of Welding Parameters on Microstructure and Mechanical Properties of Friction Stir Spot Welded of Titanium Alloy TiAl6V4

**S. Nader & M. Kasiri-Asgarani \***

Department of Materials Engineering,  
Najafabad Branch, Islamic Azad University, Najafabad, Iran  
E-mail: m.kasiri.a@gmail.com

\*Corresponding Author

**K. Amini**

Department of Mechanical Engineering,  
Tiran Branch, Islamic Azad University, Isfahan, Iran

**M. Shamanian**

Department of Mechanical Engineering,  
Isfahan University of Technology, Isfahan, Iran

**Received: 9 December 2015, Revised: 11 March 2016, Accepted: 16 April 2016**

**Abstract:** In this study, friction stir spot welding (FSSW) is applied to join the TiAl6V4 titanium alloy with 1.5 mm thickness and then the effect of rotational speed and tool dwell time on microstructure and mechanical properties is investigated. In this regard, the speed of the tool rotation was considered as 800, 1000, and 1200 rpm, as well as the tool dwell time was set at 7 and 12s. Microstructural evaluation was carried out using optical microscopy (OM) and scanning electron microscopy (SEM). In addition, tensile-shear and hardness studies were performed to analyze mechanical properties. The obtained results from microstructural evaluation show that the welded joints consist of two regions, namely the SZ and the HAZ-regions. Additionally, microstructure of the SZ-region was identified in the form of  $\alpha/\beta$  layer within the initial  $\beta$ -phase. The results of tensile/shear tests and micro-hardness test indicated that the joint strength and hardness are enhanced with increasing the rotational speed and dwell time. The tensile/shear strength is increased from 2.7 to 15 KN with increasing the rotational speed at constant dwell time of 7s, and also is increased from 7.3 to 17.25 KN with increasing the rotational speed at constant dwell time of 12s. The maximum tensile/shear strength was achieved for the welded joint with the dwell time of 12s and rotational speed of 1250 rpm. The hardness of SZ, HAZ regions and base metal are measured around 380 to 420, 340 to 380, and 300 to 340, respectively.

**Keywords:** Dwell Time, Friction Stir Spot Welding, Rotation Speed, Titanium Alloy

**Reference:** Nader, S. Kasiri Asgarani, M., Amini, K., and Shamanian, M., "Effect of Welding Parameters on Microstructure and Mechanical Properties of Friction Stir Spot Welded of Titanium Alloy TiAl6V4", Int J of Advanced Design and Manufacturing Technology, Vol. 9/No. 2, 2016, pp. 93-100.

**Biographical notes:** **S. Nader** received his MSc in Materials Engineering from University of IAU, Najafabad Branch, Isfahan, Iran. **M. Kasiri** is an assistant professor in Materials Engineering at Najafabad Branch, IAU. **K. amini** is an associate professor in Materials Engineering. **M. Shamanian** is a professor in Materials Engineering at Isfahan University of Technology.

## 1 INTRODUCTION

Titanium and its alloys belong in the rank of the new materials engineering and have been used as industrial metals since 1940. Due to their favorable physical, chemical, and mechanical properties, they could find unique applications. In order to have a high ratio of strength to weight, high corrosion resistance, and biocompatibility with the human body, titanium alloys have been widely utilized in the aerospace, nuclear, marine, chemical, and medical industries. Fabrication of titanium alloys with traditional fusion welding methods causes the formation of brittle microstructures, severe distortion, residual stresses, and welding defects. The presence of these problems leads to the joining of titanium alloys by solid-state welding methods. In these types of welding methods, the melting pool is not created and it is not necessary to protect and control the melting pool [1].

Friction stir welding (FSW), as a newly-developed solid-state joining technology, was invented by TWI in 1991 and it is suitable to produce titanium welded joints without any fusion welding defects. There are many advantages of FSW compared to the fusion welding methods, including its ease to work, low cost of equipment, ability to automation, high quality of welds, minimum residual stresses and distortion, and the desired mechanical properties which are near to the base metal [2]. Friction stir spot welding (FSSW) as a useful alternative to resistance spot welding (RSW) was invented and used by Mazda motor and Kawasaki heavy industrial companies in 2001 [3].

In this method, a rotational tool penetrates into the overlap plates and after a short stop, it is pulled out. When the tool rotates within two plates, a stir zone (SZ) including dynamic recrystallization materials is formed. With the pulling out of tool and the completion of the joining function, the keyhole is remained in the weld. The keyholes can be filled using special tools and fixtures [4]. Many researches have been performed on the FSSW of aluminum alloys which have various applications in the aerospace, marine and transportation industries. However, the FSSW of titanium alloys is rarely considered. This can be attributed to the existence of many challenges in the FSSW process of titanium alloys.

As an example, some of these challenges include high working temperature, the need to protect the weld region against the environment atmosphere, the need to precise controlling of the process parameters in order to obtain the required temperature during process, and the selection of the tool materials [5-7]. Process parameters of the FSSW affect the weldments microstructure. Some of these parameters are the tool geometry, rotational speed, dwell time, vertical force, depth of

penetration, and surface preparation. Therefore, in this research, the effect of tool rotational speed and dwell time on microstructure and mechanical properties of friction stir spot welded of titanium alloy TiAl6V4 are investigated.

## 2 EXPERIMENTAL DETAILS

### 2.1. Materials

TiAl6V4 titanium alloy sheets with 1.5 mm thickness were selected for the present research. Their chemical composition is listed in Table 1.

**Table 1** Chemical composition of the Ti-6Al-4V alloy used in this research (wt %)

Al	V	Fe	Si	Mn	Other	Ti
6.5	4	0.14	0.02	0.03	< 0.15	89.16

### 2.2. Tool design

The tool used in welding operations was fabricated from the WC-Co based alloy. The tool dimensions are shown in Table 2 and Fig. 1.

**Table 2** The features of the tool used in this work

Pin material	WC-Co
Shoulder material	WC-Co
Type of pin	Conical (frustum)
Type of shoulder	plain
Pin diameter	6 mm (large dia.), and 3 mm (small dia.)
Pin length	1.2 mm
Shoulder diameter	14 mm

### 2.3. Preparation

All the specimens were cut from the sheets with the size of 100 mm × 25 mm. Before welding, firstly, the surfaces of the sheets were grinded by soft emery papers for removal of any oxide pollution. Secondly, for acidic cleaning treatment, the sheets were immersed in the aqueous solution of 5% HF and 45% HNO<sub>3</sub> at 5 min. After that, the cleaned sheets were immediately washed with warm water in order to get rid of any acid. Finally, the humidity of the surfaces was adsorbed using cotton cloth and they were completely dried by warm air. The cleaning treatment was carried out around 15 min before the welding process.

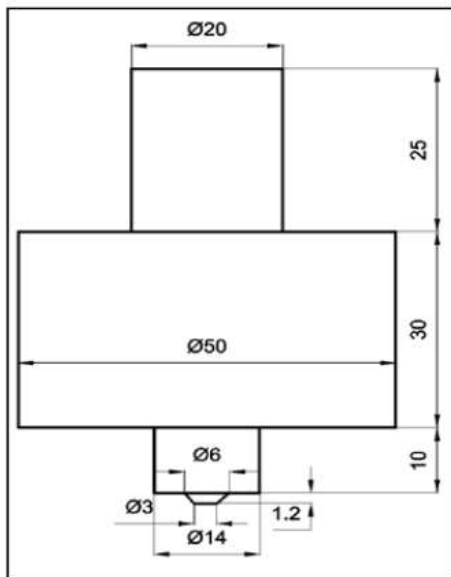


Fig. 1 Schematic of tool used in this research

#### 2.4. The welding procedure

Three different tool rotational speeds and two various dwell times were used to fabricate the joints. The welding parameters are given in Table 3. In order to protect the weld region, pure argon gas (99.99%) was utilized during the FSSW process. The welded samples were mounted with hot mounting and then they were grinded and polished by emery grid paper and diamond paste, respectively. For metallographic studies, the mounted samples were etched using kerroll's reagent: 3 ml HF, 6 ml HNO<sub>3</sub>, and distilled water. The tensile/shear specimens were machined according to the ASME standard [8]. The dimensions of tensile/shear samples are illustrated in Fig. 2. Micro-hardness test was performed on the cross-section of welds.

Table 3 Variations of the rotation speed and the tool dwell time

Sample number	Rotation speed (rpm)	Tool dwell time (S)
1	1250	12
2	1250	7
3	1000	12
4	1000	7
5	800	12
6	800	7

Vickers micro-hardness measurements were taken according to ASTM E384-11e1 [9], at 0.5 mm below the upper sheet surface with 1.0 mm interval using a diamond indenter with 100 gf load and 15s dwell time. Figure 3 shows the cross-section of the FSSW welded sample and the situation of the hardness points.

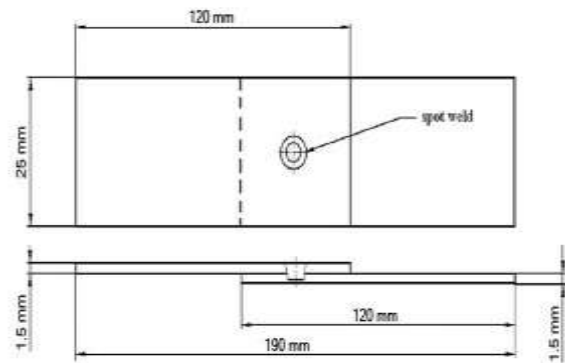


Fig. 2 Dimensions of the shear-tensile sample [8].

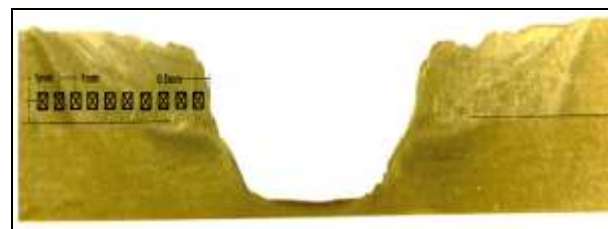


Fig. 3 Cross-section of the FSSW welded sample and schematic of hardness points

#### 2.5. The characterization equipment

Microstructures were observed using an Olympus optical microscope and a LEO 435VP scanning electron microscope. The tensile/shear tests were performed using an Instron 4486 machine at a constant crosshead speed of 2 mm/s. The Vickers micro-hardness test was carried out on a Koopa MH1 machine.

### 3 RESULTA AND DISCUSSION

#### 3.1. Qualify investigation

Due to the sensibilities of TiAl6V4 titanium alloy during welding, the first step to produce the joint is making the perfect joint. In this regard, the fabricated joint should firstly be without any defect in quality. The obtained experimental results from friction stir spot welding of TiAl6V4 titanium alloy showed that there are principally four types of defects that may occur during the FSSW process, including perforation of the sample, change in the weld color, movement of the workpiece during welding, and formation of excessive flash. Figure 4 shows the top view of a friction stir spot weld on the upper sheet of the failed specimen. The creation of all failures is related to the lack of perfect choice of welding parameters. The perforation of samples is due to the selection of insufficient pin length, and the formation of excessive flash can be

attributed to the over exposure of tool shoulder with the upper sheet. Additionally, changing of the weld color is related to insufficient protection of the weld surface, and the movement of the workpiece during welding can be attributed to the use of inappropriate fixture. Figure 5 shows the obtained perfect joints from the FSSW process. As can be seen, all of the joints are fabricated without any defects and movements.

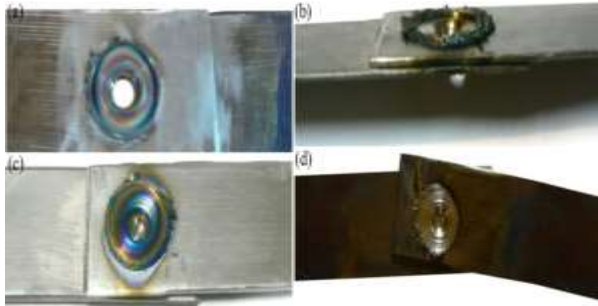


**Fig. 4** Images of the welding defects during the FSSW process (a) penetration of the sample (b) flash excessive (c) change of the color in the sample (d) movement of the sample



**Fig. 5** Images of the welded joints without any defects

### 3.2. Evaluation of various weld regions

Figure (6a) shows typical examples of the macroscopic structure of the cross-section of the welds made under the welding condition of the rotational speed of 1250 rpm and tool dwell time of 7 s. As can be seen, the cross section of the friction stir spot welded joint is divided into three regions, including the base metal (BM), the heat affected zone (HAZ), and the stir zone (SZ) shown in Fig. 6b. It is worth noting that, despite aluminum and magnesium alloys, the thermomechanical affected zone (TMAZ) disappears in the cross-section of the joint. In this regard, Fig. 6b shows a sharp interface between the SZ and the HAZ-regions, which is indicative of the absence of the TMAZ-region. The absence of the TMAZ-region is related to the notion that titanium alloys show the highest strength and lowest thermal conductivity compared to aluminum alloys. Due to the low thermal conductivity of titanium alloys, the generated heat during the FSSW process is not far from the weld region; so, the cold and relatively strong region around the weld region resists against the deformation force which is a creator of the TMAZ-region [10-13].

Concerning the created structure, it can be claimed that, the temperature of the SZ-region reaches to above the  $\beta$ -transformation temperature and consequently, the structure totally changes to the single  $\beta$ -phase. Because of the equilibrium cooling within all energy areas, the  $\alpha$ -phase nucleates homogeneously and finally, the  $\alpha/\beta$  layer is formed within the structure. Figure 9 displays the structure of the HAZ-region. Accordingly, the HAZ structure is divided into two regions which include the co-axial grain of  $\alpha$  and  $\alpha/\beta$  layer within the initial  $\beta$ -phase. The peak temperature in this region is lower than the  $\beta$ -transformation temperature and this microstructure is created by cooling from the peak temperature.

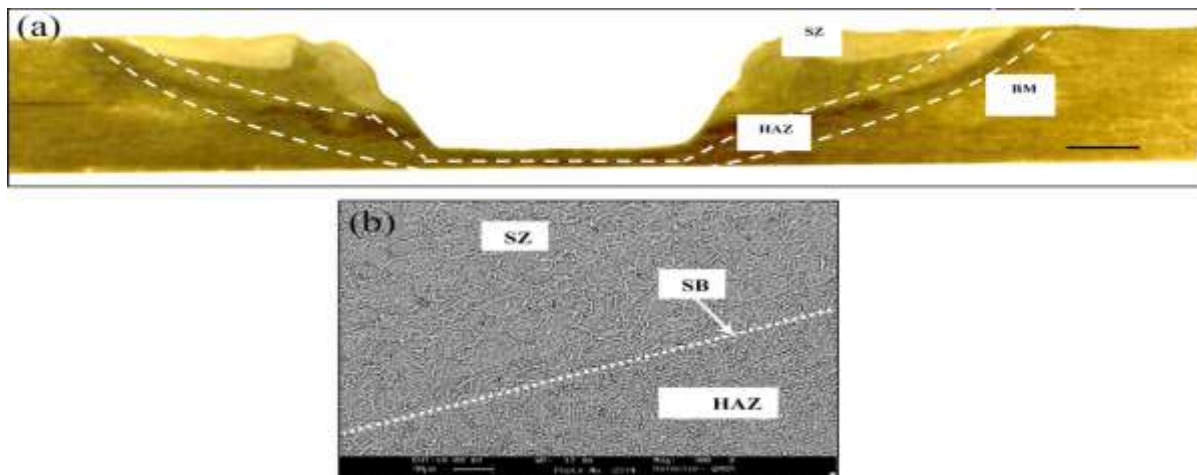


**Fig. 6** (a) Macroscopic image from the joint section (b) SEM image of the SZ and HAZ interface

This can be attributed to the fact that, during the heating step, the  $\alpha$ -phase is changed to the  $\beta$ -phase within the deformed  $\alpha/\beta$  layer. When the peak temperature is lower than the  $\beta$ -transformation temperature, the amount of remained  $\alpha$ -phase is retained within the structure and in order to reduce the energy level, the co-axial grains of  $\alpha$ -phase are formed in the structure [10].

### 3.3. Grain and microstructure characterization of the base metal

Figure 7 shows the optical and the SEM images of the base metal.

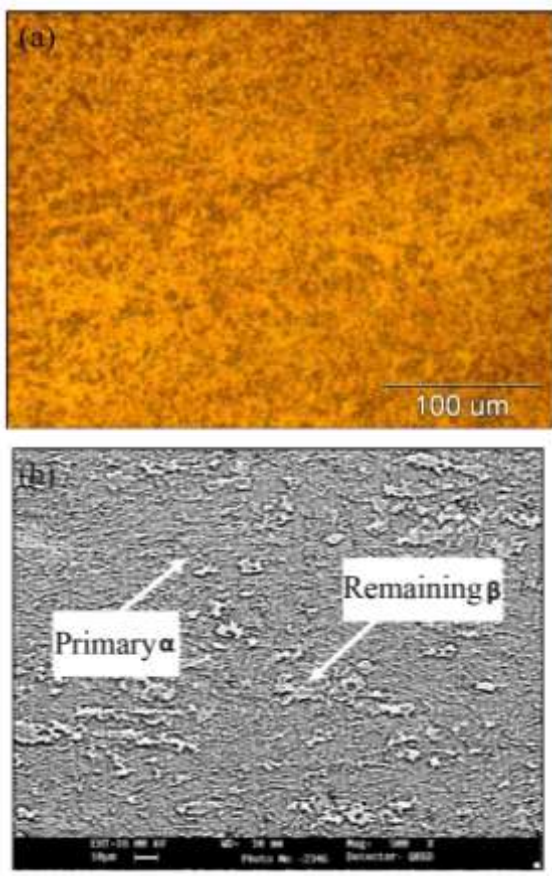


Fig. 7 Microstructure of the base metal (a) optical microscopy (b) SEM micrograph

As can be seen, microstructure of the base metal includes primary  $\alpha$ -phase and remained  $\beta$ -phase. In the SEM image, the  $\alpha$ -phase and  $\beta$ -phase are appeared as the dark and white-regions, respectively. The color of the  $\alpha$ -phase and  $\beta$ -phase in the optical image is in contrast with the SEM image. Figure 8 depicts the SEM image of the SZ-region structure in sample 1 at two magnifications. According to Fig. 7, the microstructure

of the SZ-region consists of the  $\alpha/\beta$  layer within the initial  $\beta$ -phase.

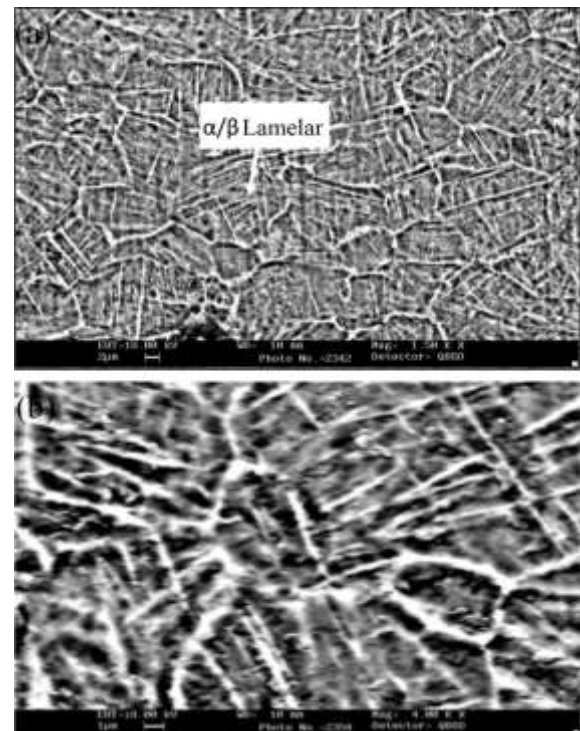


Fig. 8 SEM micrographs of the SZ- region in sample 1 (a) 1500X (b) 4000X

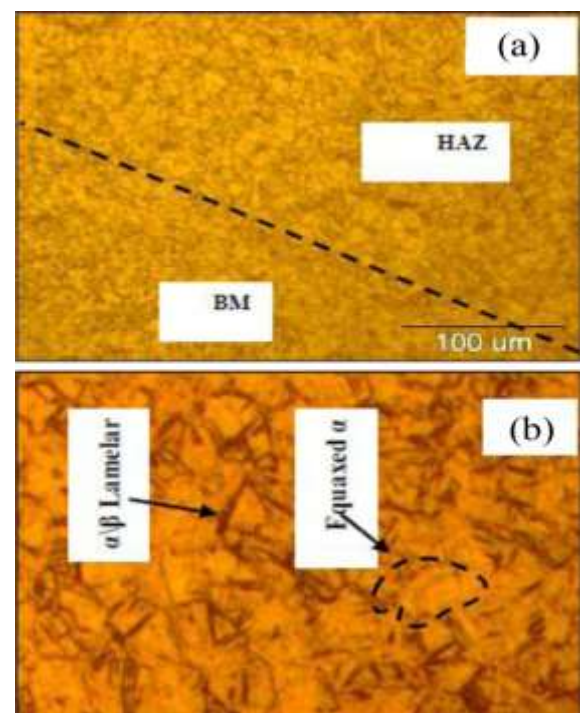
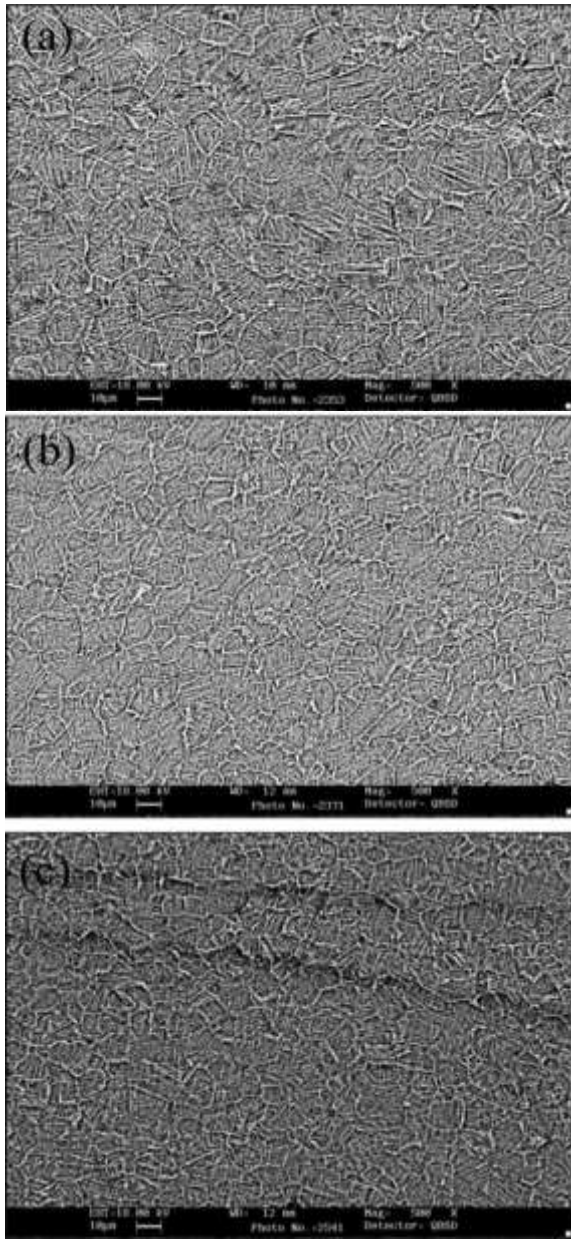


Fig. 9 Optical image of sample 3 (a) interface of BM and HAZ (b) the HAZ structure

### 3.4. Effect of rotational speed and dwell time on microstructure

Figure 10 shows the SEM image of SZ-region of the welds made at the welding conditions of the rotational speeds of 800, 1000, 1250 rpm and dwell time of 12 s. As can be seen, the grain size increases in the structure with increasing the rotational speed.



**Fig. 10** SEM micrographs of the SZ- region in samples (a) 1 (b) 3 (c) 5 at the tool dwell time of 12 s and rotation speeds of 800,1000,1250 rpm

It is obvious that during the FSSW process, the temperature of the stir zone reaches to above the  $\beta$ -transformation temperature and with increasing the rotation speed, the fine grains will change into the

coarse grains. Similarly, at the constant rotation speed, the heating input also increases with increasing the tool dwell time and again lead to the formation of a coarse structure [14-15]. Figure 11 shows the relationship between the rotation speeds with grain size. It is obvious that with increasing the rotation speed and tool dwell time, the structure will be coarsened.

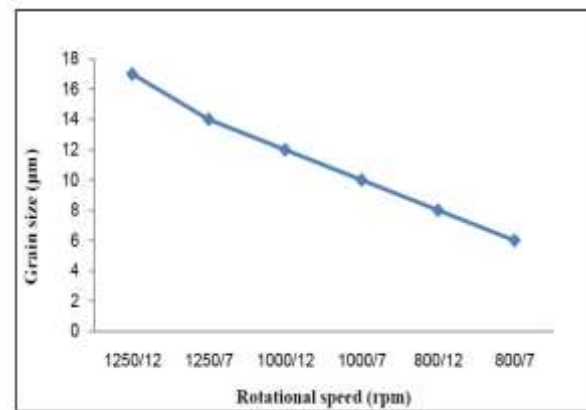


**Fig. 11** Comparison between variations of grain size and rotational speed in the welded joints

### 3.5. The tensile/shear test

In order to investigate the welded joint strength, the tensile/shear test is performed. The obtained results of tensile/shear test are shown in Table 4. It is clear that the welded joint at the rotation speed of 1250 rpm and the tool dwell time of 12 s shows the highest strength among the fabricated joints. At the constant of rotational speeds, with increasing tool dwell time from 7 to 12s, the shear strength increases from 5.25 KN to 15.9 KN. This can be attributed to the increase of the width of the stir region due to the prolongation of the welding time. The expansion of the stir-region leads to the formation of the  $\alpha/\beta$  layer, resulting in the increase of the shear-tensile strength. The obtained results are in good agreement with the results of other researchers [7].

In addition, at constant tool dwell time, with increasing the rotational speed, the shear strength increases as well. The diameter of the weld nugget increases with increasing the rotational speed due to the increase of the welding heat input. The increase of the weld nugget diameter can cause the fracture of higher force in high rotation speed. In other words, some researchers [10] show that the grain size of the initial  $\beta$ -phase is the most important affecting parameters on the mechanical properties of Ti-6Al-4V alloy. With increasing the rotational speed and tool dwell time, the heating input increases, leading to the increase of the grain size of the initial  $\beta$ -phase. The increase of the grain size of initial  $\beta$ -phase results in the increase of the amount of the  $\alpha/\beta$  layer and the shear strength.

### 3.6. Hardness

Figure 12 shows the hardness profile of specimens with the numbers of 2, 4, and 6 as opposed to the base metal. It is clear that, in all of the welded joints, the hardness of the SZ-region is higher than the hardness of the HAZ-region and the hardness of the base metal is the lowest.

This can be attributed to the formation of plastic deformation in the SZ-region and also finer structure due to the formation of dynamic recrystallization in the SZ-region compared with the base metal. The finer structure causes the increase of strength and hardness within the SZ-region.

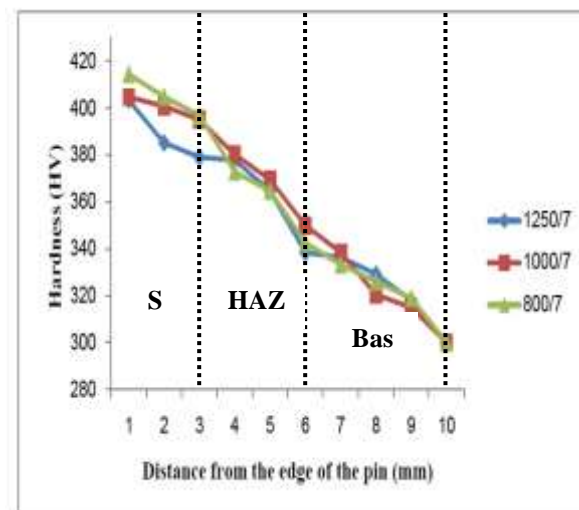


Fig. 12 Comparison between variations of hardness and distance from the pin edge in samples 2, 4 and 6.

Table 4 The obtained results of the shear-tensile test

No.	Rotation speed (rpm)	dwell time (S)	Shear-tensile force (KN)	Type of Fracture	Fracture area
1	1250	12	17.25	Pull out	HAZ
2	1250	7	15	Pull out	HAZ
3	1000	12	15.9	Pull out	HAZ
4	1000	7	5.25	interfacial	SZ
5	800	12	7.3	Pull out	SZ
6	800	7	2.7	interfacial	SZ

## 4 CONCLUSION

1. During the FSSW process of the Ti-6Al-4V alloy, the weld region is divided into two regions: the SZ-region and the HAZ-region. However, the TMAZ-region disappeared in the weld region.
2. The SZ-structure includes the  $\alpha/\beta$  layer within the initial  $\beta$ -phase. Consequently, it was clear that the peak temperature in the SZ-region was higher than the  $\beta$ -transformation temperature.
3. The dual-phase structure was formed in the HAZ-region. It included co-axial  $\alpha$ -phase grains and the  $\alpha/\beta$  layer within the initial  $\beta$ -phase. As a result, the peak temperature in the HAZ-region was lower than the  $\beta$ -transformation temperature.
4. With increasing the rotational speed and the tool dwell time, the heating input increased in the welded

joint and it caused the increase of the grain size of the initial  $\beta$ -phase, and consequently led to coarse microstructure.

5. The tensile/shear strength is increased from 2.7 to 15 KN with increasing the rotational speed at constant dwell time of 7s, and also it is increased from 7.3 to 17.25 KN with increasing the rotational speed at constant dwell time of 12s. The highest shear-strength was obtained during the tool dwell time of 12 s, compared with the tool dwell time of 7 s. In addition, the highest shear strength belonged to a welded joint made by the rotational speed of 1250 rpm.
6. In all welded joints, the hardness of SZ, HAZ regions and base metal are measured around 380 to 420, 340 to 380, and 300 to 340, respectively. The SZ-region showed the highest hardness compared with the base metal. Indeed, the hardness in the HAZ-region was higher than the base metal.

**REFERENCES**

- [1] Aghajani, H., Elyasi, M., and Hoseinzadeh, M., "Feasibility study on Aluminum alloys and A441 AISI Steel joints by friction stir welding", *International Journal of Advanced Design and Manufacturing Technology*, Vol. 7, No. 4, 2014, pp. 99-109.
- [2] Fari, A., Batalha, G. F., Prados, E. F., Magnabosco, R., and Delijaicov, S., "Tool wear evaluations in Friction stir processing of commercial Titanium Ti-6Al-4V", *Wear*, Vol. 302, 2012, pp. 1327-133.
- [3] Kurtulmus, M., "Friction stir spot welding parameters for Polypropylene sheets", *Scientific Research and Essays*, Vol. 7, 2012, pp. 947-956.
- [4] Kemal Bilici, M., "Application of taguchi approach to optimize FSSW parameters of Polypropylene", *Materials and Design*, Vol. 35, 2012, pp. 113-119.
- [5] Ramirez, A. J., Juhas, M. C., "Microstructural evolution in Ti-6Al-4V friction stir welds", *Materials Science Forum*, Vols. 426-432, 2003, pp. 2999-3004.
- [6] Nader, S., Kasiri, M., and Shamanian, M., "Effect of dwell time on microstructure of friction stir spot welded of titanium alloy TiAl6V4", *Advanced Processes in Materials Engineering*, Vol. 9, No. 2, 2015, pp.149-156.
- [7] Feng, Z., Santella, M. L., and David, S. A., "Friction stir spot welding of advanced high-strength steels a feasibility study", *Transactions Journal of Materials and Manufacturing*, Vol. 114, 2005, pp. 1-7.
- [8] ASME Standard, Section IX, "Welding, brazing and fusing qualification", QW-462.9, 2007 Edition.
- [9] ASTM: E384-11e1, "Standard test method for knoop and vickers hardness of materials".
- [10] Zhang, Y., Sato, Y., Kokawa, H., Park, S.C., and Hirano, S., "Microstructural characteristics and mechanical properties of Ti-6Al-4V friction stir welds", *Material Science and Engineering: A*, Vol. 485, 2007, pp.448-445, 2007.
- [11] Liu, H. J., Zhou, L., and Liu, Q. W., "Microstructural characteristics and mechanical properties of friction stir welded joints of Ti-6Al-4V titanium alloy", *Materials and Design*, Vol. 31, 2009, pp. 1650-1655.
- [12] Zhou, L., Liu, H. J., and Liu, Q. W., "Effect of rotation speed on Microstructure and mechanical properties of Ti-6Al-4V Friction Stir Welded Joints", *Materials and Design*, Vol. 31, 2010, pp. 2631-2636.
- [13] Lee, W. B., Lee, C. Y., and Chang, W. S., "Microstructural investigation of friction stir welded pure titanium", *Material Letters*, Vol.59, 2005, pp. 3315-3318.
- [14] Mishra, R. S., Ma, Z. Y., "Friction stir welding and processing", *Material Science and Engineering: R*, Vol. 50, 2008, pp. 1-78.
- [15] Rai, R., De, A., Bhadeshia, H. K. D. H., and Debroy, T., "Review: Friction stir welding tools", *Science and Technology of Welding and Joining*, Vol.16, 2011, pp. 325-342.